

Quantifying seismic survey reverberation off the Alaskan North Slope

Melania Guerra, Aaron M. Thode, and JJFSusanna B. Blackwell and JJFA. Michael Macrander and JJF

Citation: *J. Acoust. Soc. Am.* **130**, (2011); doi: 10.1121/1.3628326

View online: <http://dx.doi.org/10.1121/1.3628326>

View Table of Contents: <http://asa.scitation.org/toc/jas/130/5>

Published by the [Acoustical Society of America](#)

Quantifying seismic survey reverberation off the Alaskan North Slope

Melania Guerra^{a)} and Aaron M. Thode

Marine Physical Laboratory, Scripps Institution of Oceanography, University of California San Diego,
La Jolla, California 92093-0238

Susanna B. Blackwell

Greeneridge Sciences, Incorporated, 6160-C Wallace Becknell Road, Santa Barbara, California 93117

A. Michael Macrander

Shell Exploration and Production Company, 3601 C Street, Suite 100, Anchorage, Alaska 99503

(Received 4 January 2011; revised 23 June 2011; accepted 1 August 2011)

Shallow-water airgun survey activities off the North Slope of Alaska generate impulsive sounds that are the focus of much regulatory attention. Reverberation from repetitive airgun shots, however, can also increase background noise levels, which can decrease the detection range of nearby passive acoustic monitoring (PAM) systems. Typical acoustic metrics for impulsive signals provide no quantitative information about reverberation or its relative effect on the ambient acoustic environment. Here, two conservative metrics are defined for quantifying reverberation: a minimum level metric measures reverberation levels that exist between airgun pulse arrivals, while a reverberation metric estimates the relative magnitude of reverberation vs expected ambient levels in the hypothetical absence of airgun activity, using satellite-measured wind data. The metrics are applied to acoustic data measured by autonomous recorders in the Alaskan Beaufort Sea in 2008 and demonstrate how seismic surveys can increase the background noise over natural ambient levels by 30–45 dB within 1 km of the activity, by 10–25 dB within 15 km of the activity, and by a few dB at 128 km range. These results suggest that shallow-water reverberation would reduce the performance of nearby PAM systems when monitoring for marine mammals within a few kilometers of shallow-water seismic surveys. © 2011 Acoustical Society of America. [DOI: 10.1121/1.3628326]

PACS number(s): 43.80.Ev, 43.80.Nd [JJF]

Pages: 3046–3058

I. INTRODUCTION

The Beaufort Sea borders the Alaskan North Slope along a 340 km swath of northern Alaska. The continental shelf along this coast is relatively narrow, between 60 and 120 km. Its depth can reach a few hundred meters, but in this paper a “shallow-water environment” will refer to continental shelf water depths of 50 m or less. The Beaufort Sea, along with the adjacent Chukchi Sea, is home to a variety of whales, seals and other marine mammals that may be sensitive to the sounds of increasing industrial activities in the area.

During the ice-free months of 2006–2009 multiple overlapping anthropogenic activities by several independent companies and government agencies were conducted in this region. Of particular concern to regulators are sounds originating from seismic airgun surveys (Barger and Hamblen, 1980; Greene and Richardson, 1988). Quantifying the potential long-term impacts of these surveys on the viability of marine mammal populations faces numerous challenges, beginning with the problem of defining the relevant measurement metrics. Some consensus is emerging about metrics of impulsive signals that are appropriate in terms of estimating auditory injury to animals (Madsen, 2005; Southall *et al.*, 2007; Kastak *et al.*, 2005). These measurements include

peak-to-peak amplitude, root-mean-square (rms) amplitude, and sound exposure (SE) (Urick, 1983; Madsen, 2005). Limited laboratory data on marine mammal hearing, reviewed in Southall *et al.* (2007), suggest that sound exposure level (SEL) in particular, may be a biologically relevant metric for predicting the degree of temporary and permanent threshold shift in individuals exposed to high-intensity sounds; however, there has been little research on the long-term impacts of chronic acoustic exposure on marine mammal populations, nor are there formal regulations for quantifying communication masking effects in marine mammals.

In shallow-water environments additional factors arise when characterizing the sounds from a seismic airgun survey. In shallow water no direct path exists between the airgun source and a receiver; instead, the pulse energy arrives as a series of multipath (normal mode) arrivals, each with a different arrival time at the receiver. Due to frequency-dependent geometric dispersion effects, the time-dependent frequency structure and duration of each modal multipath arrival changes, complicating attempts to estimate the biologically relevant sound exposure. A portion of the pulse energy also travels through the ocean floor and re-emerges into the water column as a head wave, which can provide a significant fraction of the total signal energy below 50 Hz.

Yet another consequence of shallow-water propagation is the substantial reverberation that follows all modal arrivals. As the pulse propagates through shallow water, it interacts multiple

^{a)}Author to whom correspondence should be addressed. Electronic mail: melania@mpl.ucsd.edu

times with the ocean surface, bottom, and substrate, scattering energy incoherently throughout the water column in the form of reverberation. Although the received levels of reverberation are generally lower than peak or rms measurements of the coherent arrivals, they can be greater than natural ambient noise levels. Reverberation can persist over timescales much longer than the duration of the dispersed coherent arrivals, even persisting until the start of the next seismic airgun shot. Thus, seismic airgun reverberation can continuously elevate the background noise field during a survey, even during times between airgun shots. In general, modeling or predicting reverberation is difficult; reverberation characteristics are highly dependent on the local bathymetry and propagation environment.

The presence of reverberation in shallow water has two important consequences when trying to understand the potential impact of seismic airgun activities on marine mammals. First, the elevated background noise levels arising from reverberation would be expected to reduce the range at which passive acoustic monitoring (PAM) systems could detect and localize marine mammal sounds near shallow-water seismic airgun activities. Second, seismic airgun reverberation may reduce the “communication space” between animals like the bowhead whale, and thereby impact quantitative estimates of information masking (Richardson *et al.*, 1986; Clark *et al.*, 2009; Di Iorio and Clark, 2009). Thus simple metrics are desired to quantify how reverberation increases background noise above ambient levels in shallow water. This paper defines two metrics: a minimum level metric (MLM) and a reverberation metric (RM). The former simply reports the minimum sound levels detected over a given time window, while the latter estimates how much seismic airgun reverberation increases background noise over what would have existed in the absence of such activity. For the continental shelf off the Alaskan North Slope, the RM is derived from wind speed estimates obtained from satellite observations, which are then used to empirically model what wind-driven ambient noise levels would have been at a specific location. These modeled ambient levels are then compared with the MLM to generate the RM. The RM is a conservative measure of the contribution of reverberation to the background noise environment because it only applies to times when reverberation is continuously present. The RM does not apply to situations where reverberation is present, but fades away to ambient levels between airgun shots.

Section II gives details about the data used for this analysis: acoustic recordings obtained in 2008 at a variety of

ranges from seismic airgun activities off the North Slope of Alaska. Section III defines the two metrics in detail and discusses the global database used to estimate sea surface wind speeds derived from satellite data. Section IV applies these metrics to the data described in Sec. II producing information about the temporal and spatial distribution of reverberation generated by a seismic airgun survey operating between 2–128 km from acoustic receivers.

II. DATA DESCRIPTION

A. Seismic airgun survey

The reverberation data presented here arose from a seismic airgun survey generated from the M/V Gilavar in the Beaufort Sea in 2008. The Gilavar towed two WesternGeco arrays of Bolt airguns (Ireland *et al.*, 2009) approximately 275 m behind the vessel. Each array consisted of 24 airguns, distributed into three sub-arrays of 1049 in.³ volume each, for a total volume of 3147 in.³ operated at an air pressure of 2000 psi. Full airgun operations were preceded by ramp-up procedures, during which marine mammal observers (MMO) visually searched the surrounding area for evidence of marine mammal presence. During standard operation airguns were shot at intervals of 25 m (~9 s) while the vessel traveled at speeds between 4 and 5 knots. The seismic survey vessel usually rastered across a region, moving in a straight line over an area of interest, then making a 180° turn and shooting another line parallel to the previous course. During the process of turning the vessel around, activity is reduced to a mitigation-gun condition, when only one of the airguns remains active at a volume of 30 in.³.

B. Passive acoustic data

Between August 11th and October 9th 2008 a network of 40 Directional Autonomous Seafloor Acoustic Recorders (DASARs-C08) (Greene *et al.*, 2004) were deployed offshore in the Alaskan Beaufort Sea, covering a coastal distance of approximately 280 km (174 mi) between the village of Kaktovik in the east and Harrison Bay in the west (Fig. 1). DASARs were deployed on the seafloor at depths between 15 and 54 m, and were arranged into five groups, or “sites” labeled 1–5 from west to east. Each site is configured into an extended array of seven DASARs, labeled A–G from south to north, with the instruments placed at the vertices of equilateral triangles of sides 7 km in length. Site 1 had the shallowest mean

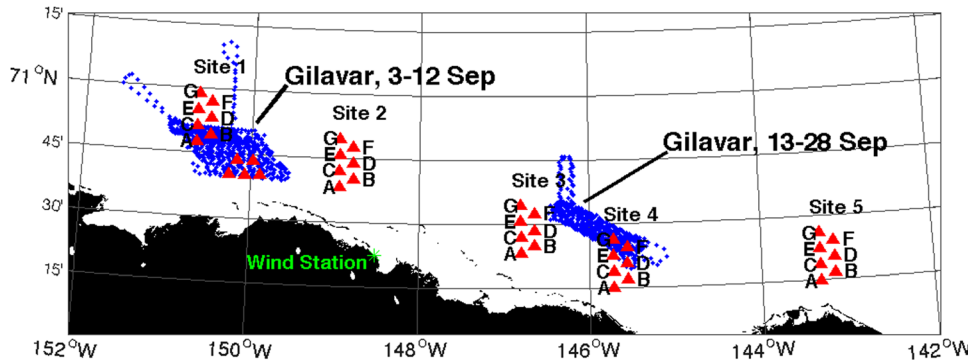


FIG. 1. (Color online) Location of DASAR deployments, arranged by site, plotted alongside with tracks and dates of extended seismic airgun surveys. Within each site DASARs are labeled A–G from south to north. The location of the Prudhoe Bay land-based wind station is also marked.

water depth of all the sites (20.5 m) while site 5 had the deepest (48.9 m). The DASARs recorded continuously at a sampling rate of 1 kHz, and the sensitivity of the omni-directional (pressure) hydrophone was -149 dB re $1 \mu\text{Pa}/\text{V}$, with a high-pass frequency response of around 20 dB per decade, in order to pre-whiten the expected ambient noise spectrum. To recover the calibrated time series, the data were passed through a single-pole IIR low-pass filter cascaded with a Butterworth high-pass filter with a 10 Hz cutoff frequency. The low-frequency cutoff was chosen to remove the effects of flow noise, as well as seismic interface and head waves. While IIR filters can be unstable, producing “ringing” in response to a large-amplitude impulsive signal, a review of the calibrated vs un-calibrated data confirmed that the reverberation data reported here are not filtering artifacts.

Figure 1 illustrates the track lines of the M/V Gilavar plotted alongside the DASAR locations, revealing two bouts of concentrated survey activity. One bout occurred around site 1 from September 3rd through the 12th, 2008, and the second bout occurred between sites 3 and 4, from September 13th through the 28th, 2008. The analyses that follow incorporate data from the shallowest (A) and deepest (G) DASARs at all sites within those date ranges. Reverberation from other DASARs at intermediate depths at a site generally lay between the levels obtained from the A and G DASARs. The land-based weather station at Prudhoe Bay, marked on Fig. 1, was used to confirm wind speeds downloaded from satellite scatterometry databases (Zhang *et al.*, 2006). The closest DASAR to the weather station was 2A.

III. ANALYSIS PROCEDURE

A. Review of fundamental level metrics

The metrics defined in this paper are intended to complement the concepts of sound exposure level (SEL) and root-mean-square (rms) sound pressure level (SPL) of a transient sound, in that they provide additional information not captured by these metrics. However, the metric definitions originate from SEL and SPL, and so their definitions are reviewed here.

The term sound exposure (SE), with units of $\text{Pa}^2\text{-s}$, is frequently used as a proxy for energy flux density. Studies of mammalian ears (Young and Wenner, 1970; Yost, 1994; Madsen, 2005) suggest that, for signals of relatively short duration (under 1 s) their perception of loudness is based on both the intensity and the duration of a received signal. However, SE is not a direct measure of the physical energy flux density, because measuring the true energy flux would require an independent measurement of acoustic particle velocity (D'Spain *et al.*, 1991). Following the definitions from Southall *et al.* (2007) and Madsen (2005), the SE of an equalized transient pulse at a given absolute time index i is computed as follows:

$$\text{SE}_i(t) = \int_{T_{i-1}}^T [p^2(t)] dt_i = \int_{f_1}^{f_2} |p(f)|^2 df \approx \sum_{k=k_1}^{k_2} \frac{|\hat{P}(k)|^2}{NF_s}, \quad (1)$$

where $p(t)$ refers to a band-limited pressure time series, i indicates the time index defined over a period $\Delta T_i = T_i - T_{i-1}$, and $P(f)$ is the analytic Fourier transform of $p(t)$, with $p(t)$ set to zero outside the time interval defined here. The second equality is a consequence of Parseval’s theorem. The third approximate equality shows how the SE is computed from the fast Fourier transform (FFT) $\hat{P}(k)$, derived from N samples of a pressure time series discretely sampled F_s times per second, such that $N = \Delta T_i F_s$. Equation (1) is frequency-dependent as it implicitly assumes the pressure time series $p(t)$ has been bandpass-filtered over a specific frequency range of interest between f_1 and f_2 .

A variant of Eq. (1) subtracts an estimate of the root-mean-square background noise from $p^2(t)$ in an attempt to estimate the pressure contribution from the transient signal alone, and not the combined transient and background pressure, but when defining the new metrics here, the definition as presented in Eq. (1) will be used.

The rms sound pressure (SP) is simply the square root of SE divided by ΔT_i and has units of pressure:

$$\text{SP}_i(t) = \sqrt{\frac{1}{T_i - T_{i-1}} \int_{T_{i-1}}^{T_i} (p^2(t) dt)} \equiv \sqrt{\frac{\text{SE}_i(t)}{T_i - T_{i-1}}}. \quad (2)$$

The decibel measure of SE, the sound exposure level (SEL), is $\text{SEL}_i = 10 \log_{10}(\text{SE}_i/\text{SE}_{\text{ref}})$, with a reference quantity of $1 \mu\text{Pa}^2\text{-s}$. The rms SPL is $\text{SEL}_i = 20 \log_{10}(\text{SP}_i/\text{SP}_{\text{ref}})$, with a reference quantity of $1 \mu\text{Pa}$.

B. Minimum level metric (MLM)

This section describes how to obtain a minimum level metric (MLM) from recordings of seismic airgun surveys. The importance of the metric is that it provides a convenient approach for measuring background noise levels that exist between airgun pulses, and thus reverberation effects. In order to generate a MLM from a raw time series, three steps have to be taken, and each step requires a decision concerning the choice of a particular time scale for processing the data.

The first step is to convert the raw time series into a series of overlapping FFTs, from which SE or SP estimates can be derived using Eqs. (1) and (2); however, both equations were originally defined for deterministic impulsive signals that are clearly distinguishable from diffuse background noise within a given time interval ΔT_i . The first decision that arises when attempting to apply these definitions to stochastic signals like seismic airgun reverberation is how long a time period ΔT_i is needed to compute the SE or SP. Stated another way, what FFT length N should be selected to compute these levels? In the absence of a sharply-defined transient pulse, it is difficult to determine how long a time sample is needed to provide a SE or SP estimate of the background noise.

In this paper ΔT_i (and thus the FFT length N) is related to the estimated integration time of the mammalian hearing mechanism of concern; given the lack of such information for various species of interest, including the bowhead whale, this integration time ΔT_i is postulated to be the typical call duration from the species. For example, for a bowhead whale

the integration interval would be on the order of 1 to 2 s (Ljungblad *et al.*, 1980; Clark and Johnson, 1984). Thus a value of ΔT_i of 1.024 s will be used in Sec. IV which translates into a FFT length of 1024 points at a 1 kHz sampling rate. Having chosen the time window, a set of overlapping FFTs are calculated over the entire time series, regardless of whether or not a seismic airgun pulse is present within a particular FFT time window. The FFT snapshots are then converted into a series of SE values using the last equality in Eq. (1).

The second step in computing the MLM is averaging sequential SE or SP estimates over a short time window, in order to reduce the variance of the result. The need for this step arises from the fact that SE or SP estimates derived from a stochastic signal fluctuate over time, even if the underlying statistical distribution of the noise properties (e.g. power spectral density) remains constant.

To achieve this step, one must decide how many FFT snapshots can be averaged to generate a “well-behaved” estimate of the stochastic signal’s SE or SP. Thus a second (averaging) timescale must be determined. This new timescale estimates a time window over which certain statistical properties of the noise are assumed to be invariant, or *stationary*, an assumption that permits the SE or SP estimates generated from data from within that time window to be averaged together. In the signal processing literature, a certain kind of stationary signal is designated *wide-sense stationary* (WSS) if both the mean and autocorrelation (i.e., the first two moments) of a stochastic signal do not change over the time period in question. Roughly stated, a WSS signal maintains the same underlying power spectrum over time, and thus sequential estimates of SE or SP can be averaged.

Reverberation in an ocean waveguide is time-dependent, in that both its magnitude and spectral content clearly evolve over time as the reverberation fades away. A time window ΔT_{wss} can be identified, however, wherein the WSS assumption holds. If $\Delta T_{\text{wss}} > \Delta T_i$, then an integer number N_{samples} of adjacent or overlapping SP or SE estimates can be averaged together, reducing the variance in accordance with Welch’s method (Oppenheim, 1999). Thus, for SE measurements of background noise,

$$\overline{SE}_i = \frac{1}{N_{\text{samples}}} \sum_{j=i}^{i+N_{\text{samples}}} SE_j. \quad (3)$$

The duration of ΔT_{wss} is always less than the interval between airgun pulses, thus ensuring that some values of SE_i will have been averaged over a time window that excludes an airgun signal. In Sec. IV A a ΔT_{wss} value of 2 s is used.

The final step in computing the MLM is determining the minimum value produced by Eq. (3) over a third time window ΔT_{\min} . Completing this step requires a final decision over what timescale the minimum should be sought. Whereas the first two timescales defined relatively short time windows of 1 to 2 s, the ΔT_{\min} window generally must be much longer, encompassing several airgun pulse arrivals. Yet, the third time window cannot be chosen to be so long that it fails to capture gradual changes in the background

reverberation caused by changes in source/receiver distance and other aspects of the operation.

Therefore ΔT_{\min} is defined as the time scale over which there are no significant changes in the source/receiver range, orientation, and/or propagation environment. Once ΔT_{\min} is determined, a MLM can be defined using either SE or SP, or equivalently SEL or SPL:

$$SPL_i^{\min} = \min\{SPL_i, SPL_{i+1}, SPL_{i+2}, \dots, SPL_{i+N_{\min}}\}, \quad (4)$$

$$SEL_i^{\min} = \min\{SEL_i, SEL_{i+1}, SEL_{i+2}, \dots, SEL_{i+N_{\min}}\}, \quad (5)$$

where N_{\min} is the number of averaged samples generated by Eq. (3) that lie within the ΔT_{\min} time window. In Sec. IV A a time window of 30 min was estimated to be the interval over which reverberation levels do not change. The units of this MLM are identical to that of a standard SPL or SEL level: dB re 1 μPa for SPL, dB re 1 $\mu\text{Pa}^2\text{-s}$ for SEL.

In summary, deriving a MLM from raw acoustic data requires three steps: generating a series of time-overlapped FFT snapshots of the data, averaging adjacent snapshots together to reduce the estimate’s variance, and then selecting the minimum averaged value that occurs over a long-term time window. The three time scales that need to be defined to obtain the metric have been labeled ΔT_i , ΔT_{wss} , and ΔT_{\min} . These values represent: (1) the assumed biologically relevant energy-integration time scale of a species’ hearing mechanism, which determines the FFT length used on the data; (2) the time scale over which the noise can be considered wide-sense stationary, which determines how many SE or SP estimates can be appropriately averaged over time; and (3) the time scale over which no significant changes take place in the source-receiver separation and propagation environment, which determines the time window over which to extract the minimum level value. The final result is a time-dependent estimate of minimum background noise level that removes any contribution from transient components of the airgun signal, including all modal and substrate arrivals.

C. Reverberation metric (RM)

To convert the MLM into a dimensionless reverberation metric (RM), an independent estimate of baseline ambient sound levels must be made in the absence of seismic airgun survey activity. The dB values of these estimates are then subtracted from the dB values of the MLM to generate the RM, with an interpretation analogous to that of signal-to-noise ratio (SNR). For example, a value of 0 dB or less for the RM would indicate that the reverberation from an airgun shot decays to natural ambient levels before the next shot occurs.

Unfortunately, no universal procedure for estimating or modeling ambient noise can be recommended, because the sources of ambient noise are highly dependent on a particular location and season. Three possible methods can be suggested, all of which require assumptions behind the ambient noise mechanisms. The first method is to simply assume that the MLM values measured before the onset of a particular anthropogenic activity would have remained at that level

during the activity (temporal consistency). The second method is to measure the MLM simultaneously at two locations: one close to the anthropogenic activity, and one so distant that contributions from that activity are assumed negligible (spatial consistency). The final method assumes that the MLM can be accurately modeled using independent measurements of other environmental parameters, such as wind, rainfall, tides, levels of shipping activity, etc. (environmental consistency). The results in Sec. IV C use this third method, because empirical measurements of ambient noise in this open-water Arctic environment correlate well with local surface wind speed measurements. Winds agitate the ocean surface, creating waves, bubbles, and other physical processes that dominate the acoustic noise environment. Noise from shipping is negligible in this region. These assumptions are consistent with previous ambient noise observations in the region (Ireland *et al.*, 2009; Wenz, 1962; Fig. 2.7 of Blackwell *et al.*, 2006). The wind speeds for this work were obtained from the online NOAA Blended Sea Winds database (Zhang *et al.*, 2006), which combines scatterometer observations from multiple satellites to produce a set of global gridded wind speeds, averaged in 6 h increments and gridded with 0.25° spatial resolution in latitude and longitude. For every time increment, the wind speed values of the four grid-points closest to a given DASAR location were spatially averaged to produce a best-estimate of the wind speed at the DASAR location at that time. The dB values of the MLM were then averaged over 6 h increments (i.e., the ambient noise values are geometrically averaged) to produce a time series with the same sampling interval as the spatially averaged blended wind data. Finally, the correlation coefficient was computed between the MLM and the spatially averaged wind data, using relative time offsets of 0, 6, and 12 h, where the MLM was delayed from the wind. Peri-

ods when seismic airgun survey activities were occurring in close proximity were rejected from the regressions. The time offset that produced the best correlation was then used to compute a set of linear regressions between the blended database wind speeds and MLM, a process discussed in more detail in Sec. IV C. The dB levels of the resulting modeled ambient noise levels are then subtracted from the MLM derived for all times, including times of seismic airgun survey activity, generating the RM.

IV. RESULTS

A. Reverberation examples

Figure 2 presents representative calibrated spectrograms of seismic airgun survey impulses generated by the Gilavar in 2008, as recorded by DASARs at sites 1 and 4. All spectrograms are computed using a 256-point FFT with 75% overlap. Figures 2(a) and 2(b) show spectrograms of seismic impulses recorded at DASAR 1A, the shallowest DASAR at site 1, on September 9th at ranges of 18.5 and 6.5 km, respectively. Figure 2(a) illustrates a 60 s portion of the mitigation-gun procedure that occurs as the vessel reverses course between transects, during which only one gun fires at a volume of 30 in.³. Subplot 2(b) illustrates the received signal from the full airgun array firing 24 guns (for a total volume of 3147 in.³) at a range of 6.5 km, with pulses generated at approximately 9 s intervals. Finally, Fig. 2(c) displays a 60 s-long spectrogram of airgun pulses from the full airgun array, but recorded at the deepest DASAR of Site 4 (DASAR 4G) at a range of 17.5 km on September 25th. These spectrograms demonstrate how different source ranges affect the modal airgun arrivals. The exact nature of reverberation is highly site dependent; one can see that the power spectral

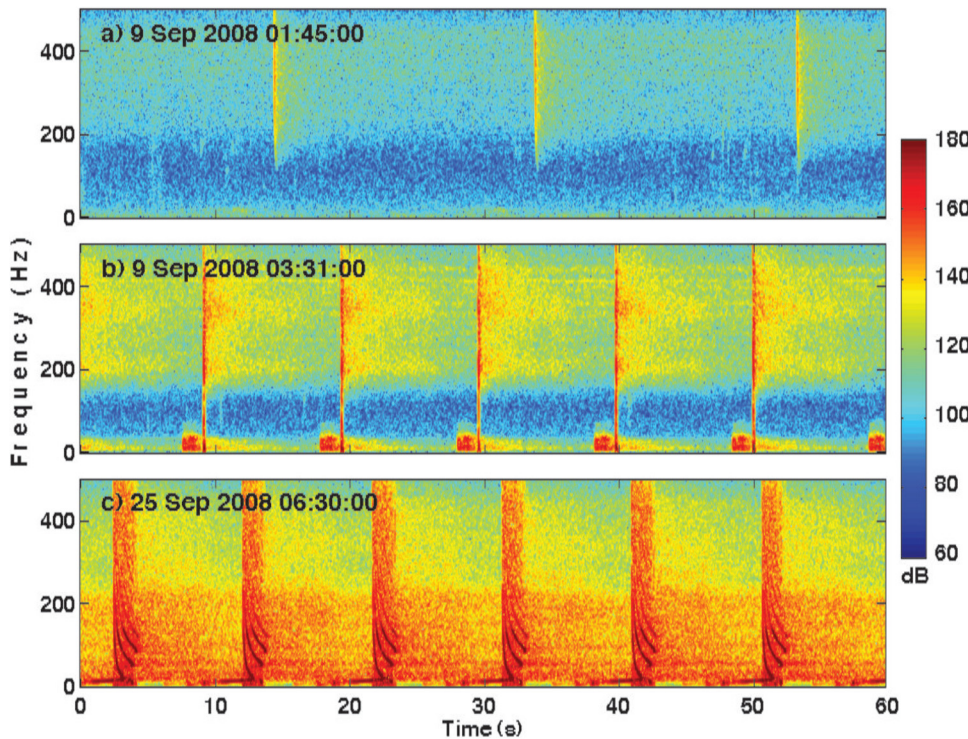


FIG. 2. (Color online) Representative spectrograms of seismic activity from the M/V Gilavar: (a) mitigation gun at 18.5 km range recorded at DASAR 1A (the shallowest DASAR at site 1) on September 9th, 2008 at 01:45; (b) full airgun array at 6.5 km range, at DASAR 1A on September 9th, 2008 at 03:31; (c) full airgun array at 17.5 km range at DASAR 4G (the deepest DASAR at site 4) on September 25th, 2008 at 06:30. The sub-50 Hz arrival visible before the main pulse arrival in (b) arises from a head-wave leaking from the substrate, and the frequency-modulated down-sweeps visible in (c) arise from the geometric dispersion of various normal mode arrivals.

density from reverberation varies from site to site, even when the same airgun source is used.

Figures 2(b) and 2(c) also show head wave arrivals from the substrate (Frisk, 1994), visible below 50 Hz.

B. Minimum level metric (MLM) estimates

Figures 3–8 display the MLM [Eq. (5)] derived for all 30-min samples of the dataset, including periods with seismic activity. To compute this metric, a series of fast Fourier transforms (FFTs) were computed, using 1024-point snapshot sizes, with 50% overlap between subsequent snapshots. A 1024-point FFT corresponds to an energy integration time ΔT_i of 1.024 s, the rough mean duration of an average bowhead whale call. The time scale ΔT_{WSS} was selected to be 2 s, and ΔT_{min} was chosen to be 1800 s, or 30 min. ΔT_{WSS} is less than the interval between seismic airgun shots (about 9 s), thus guaranteeing that some outputs of this operation will not be contaminated by energy from the direct shots visible in Fig. 2.

Figure 3(a)–3(d) shows the broadband (10–450 Hz) MLM in units of SPL, for the shallowest (A) and deepest (G) DASARs at sites 1 and 4. It is worth re-emphasizing that Fig. 3 and subsequent figures do not display any properties of the dispersed airgun pulse arrivals; instead, they quantify the reverberation that persists *between* airgun pulse arrivals. Note that the time scales in Fig. 3 cover the entire deployment period, not just times when local seismic airgun surveys are present.

The long-term broadband MLM results, shown in Fig. 3, are influenced by changes in ambient noise levels, as well as the presence of reverberation from anthropogenic sources. Substantial changes in the broadband natural ambient levels can be observed, varying by over 30 dB, but tend to occur over relatively long time scales (e.g., over the course of a day), as seen between September 14th and 19th in Figs. 3(a) and 3(b). By contrast, seismic airgun surveys produce relatively rapid fluctuations (“comb patterns”) in background levels over timescales of only a few hours, as the ship constantly varies its distance to a given DASAR while rastering across the site. This rapid variation is emphasized by the fact that the vessel reduces the number of airguns firing while it is turning around, allowing background levels to briefly return to ambient baselines, before the survey activates the full airgun array again. MLM levels at site 4 can vary by up to 30 dB, as can be seen between September 20th and 28th [Figs. 3(c) and 3(d)], as the vessel transits between the furthest and closest ranges relative to the DASAR.

Figure 4 displays the same metric as in Fig. 3, but computed for DASAR 1A only, over four 100-Hz frequency bands: 10–110, 110–210, 260–360, and 360–460 Hz. The same periods of seismic airgun activity seen in Fig. 3 can be recognized here due to the distinctive “comb pattern.” During these times, MLM values are greatest at frequencies above 260 Hz [Fig. 4(b)], regardless of vessel range and orientation to the receiver, indicating that the spectral composition of this reverberation is strongly dependent on local propagation conditions,

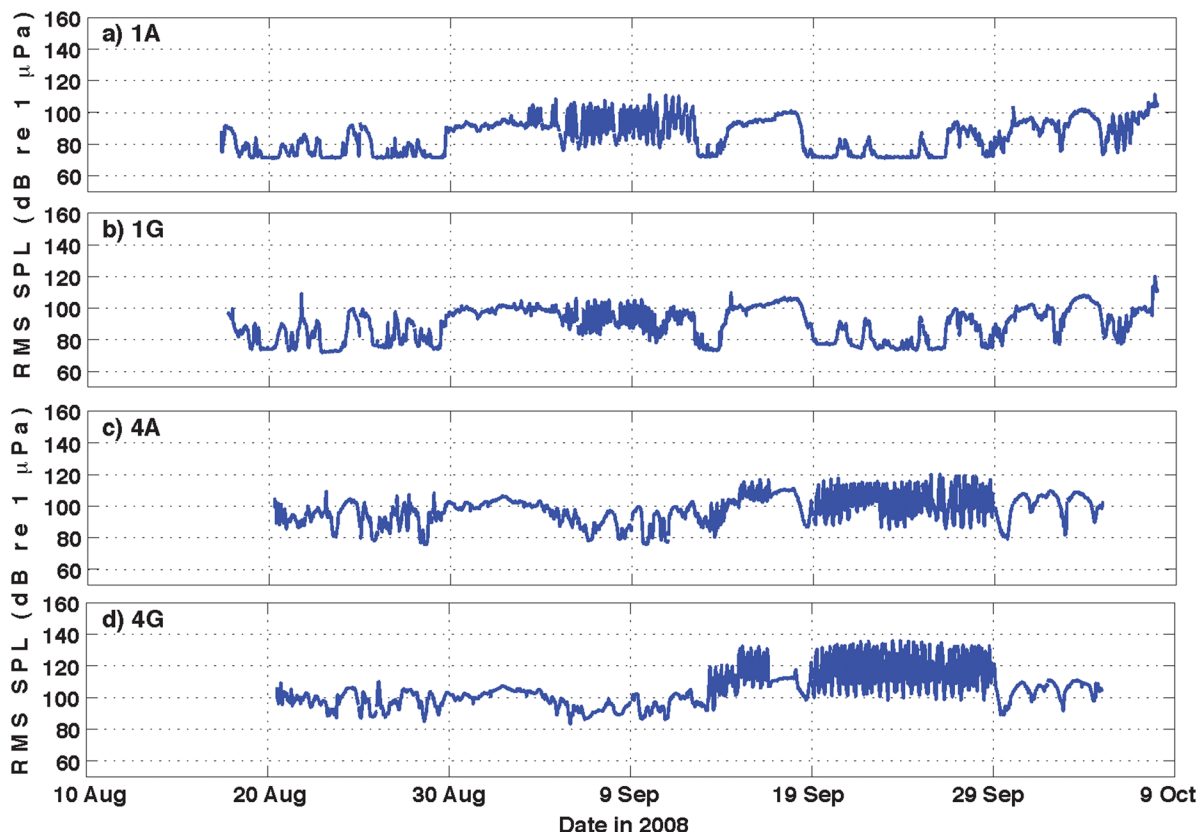


FIG. 3. (Color online) Broadband (10–450 Hz) MLM (in SPL units) at the shallowest and deepest locations of sites 1 and 4, computed for entire duration of deployment, using a 30 min long-term window: (a) DASAR 1A; (b) DASAR 1G; (c) DASAR 4A (d) DASAR 4G. DASAR A locations are the shallowest, DASAR G locations, the deepest.

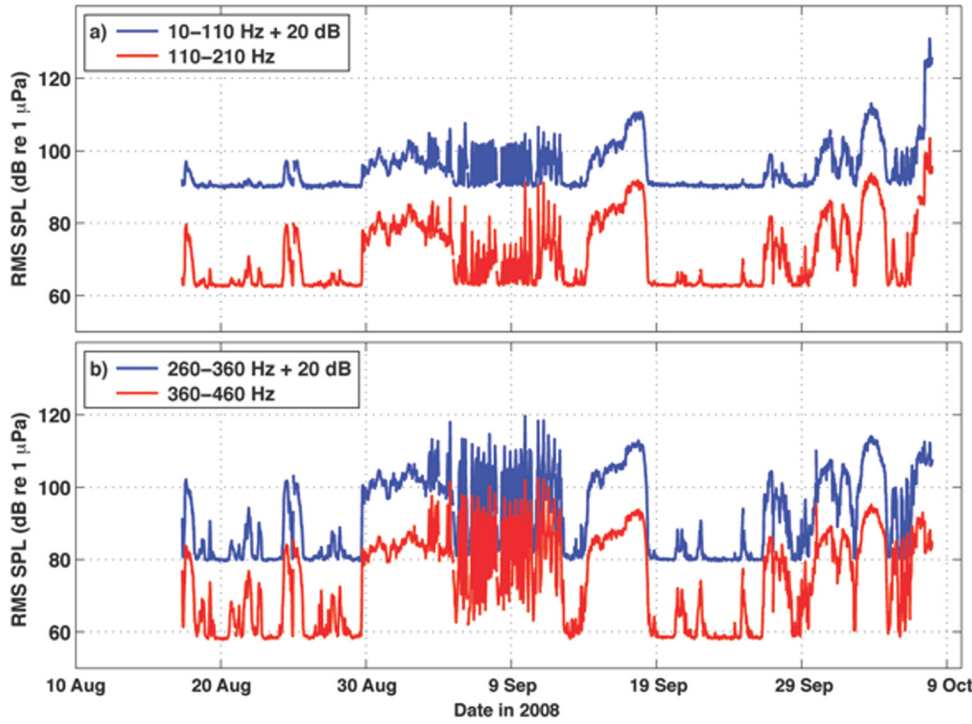


FIG. 4. (Color online) 100-Hz narrowband MLM (SPL units) for DASAR 1A, over the same timescale and using the same analysis parameters as Fig. 3: (a) 10–110 Hz and 110–210 Hz; (b) 260–360 Hz and 360–460 Hz. Note that a +20 dB offset has been applied to the upper time series.

such as local water depth. Figures 5 and 6 plot the MLM as a function of frequency, time, and location. Figure 5 plots the results obtained at the shallowest DASAR at each of the five sites (DASARs A), while Fig. 6 plots results on the same intensity scale for the deepest DASARs at each of the five sites (DASARs G). The frequency dependence has been computed over eight overlapping (50%) frequency bands between 10 and 460 Hz, each band covering a 100 Hz bandwidth.

Two one-week periods of particularly intense seismic airgun survey activity are emphasized in Figs. 7 and 8, which simply expand the time scales of Figs. 5 and 6. Figure 7

shows the MLM during the week of September 6th–14th, when the survey operated at site 1, while Fig. 8 shows the corresponding levels between September 20th and 28th, when the survey operated between sites 3 and 4. Generally, when the seismic airgun survey occurred between September 3rd and 12th in close proximity to site 1, MLM levels were more intense at the shallower DASARs, when compared to the deeper DASARs (Fig. 7). The opposite is true when the seismic airgun survey operated between sites 3 and 4: received levels of the MLM were higher at the deeper DASARs compared to the shallower DASARs (Fig. 8).

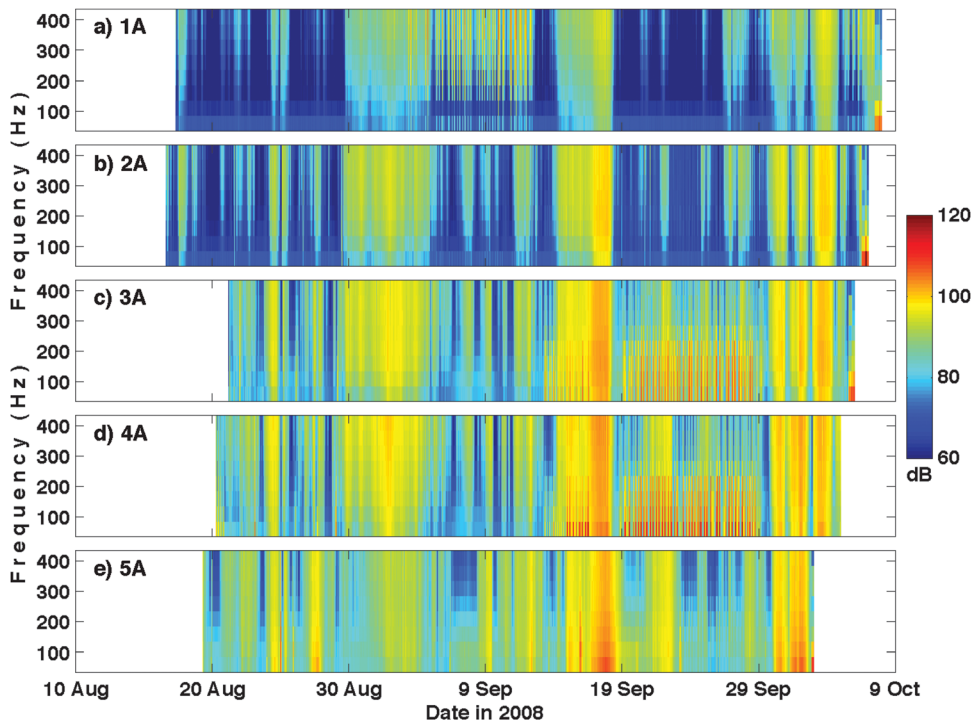


FIG. 5. (Color online) MLM (SPL units) as a function of frequency and time at shallowest locations (A DASARs) at all five sites. The metric was computed in eight frequency ranges of 100-Hz bandwidth, overlapping 50% (10–110 Hz, 60–160 Hz, 110–210 Hz, 160–260 Hz, etc.) between 10 and 460 Hz. Other analysis parameters remain the same as Figs. 3 and 4.

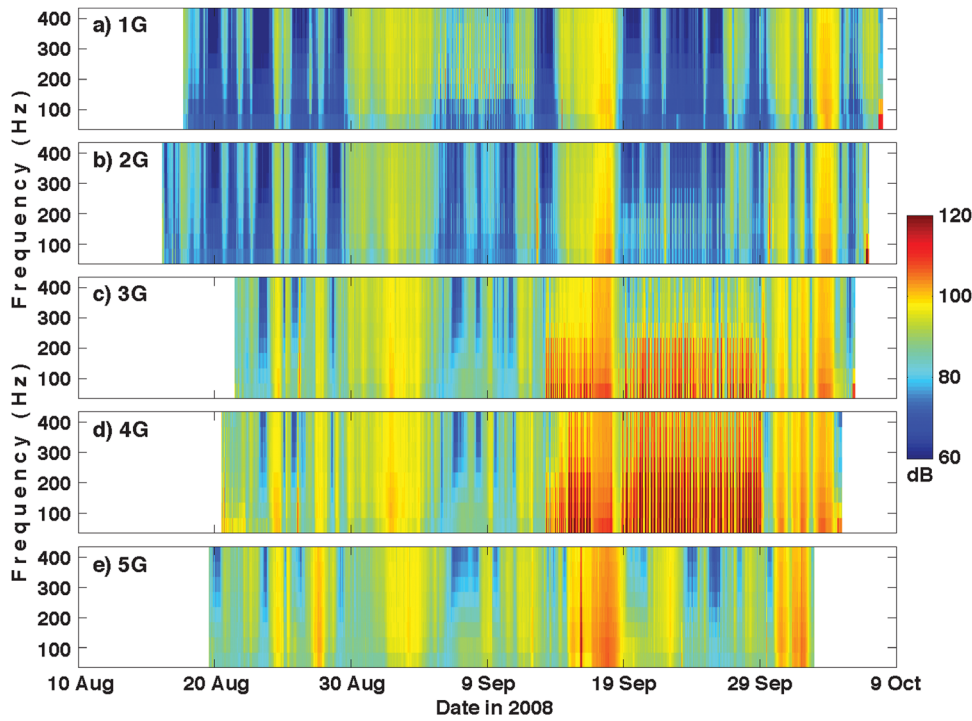


FIG. 6. (Color online) MLM (SPL units) as a function of frequency and time at deepest locations (G DASARs) at all five sites. Analysis parameters are identical to those in Fig. 5.

C. Reverberation metric (RM) estimates

As mentioned in Sec. II, the RM for this location is estimated by first empirically modeling the ambient noise using remotely-sensed wind speeds [e.g., Fig. 2.7 in (Blackwell *et al.*, 2006)].

Figure 9 illustrates the process for one particular frequency band using DASAR 2A, the shallowest DASAR (21 m depth) at site 2. Figure 9(a) plots the 6 h average of the MLM time series, calculated over the frequency band

60–160 Hz. Figure 9(b) plots the 6 h average of wind speed (in m/s) obtained from the Sea Winds database, using a $0.5^\circ \times 0.5^\circ$ area (four closest grid-point values averaged together) around the coordinates of 2A. The times between September 3rd and 12th in the time series correspond to periods when seismic airgun activity is occurring, so these periods are excluded from the correlation. The correlation coefficient between the MLM and wind speed are illustrated by the graphical matrix in Fig. 9(c) as a function of frequency band

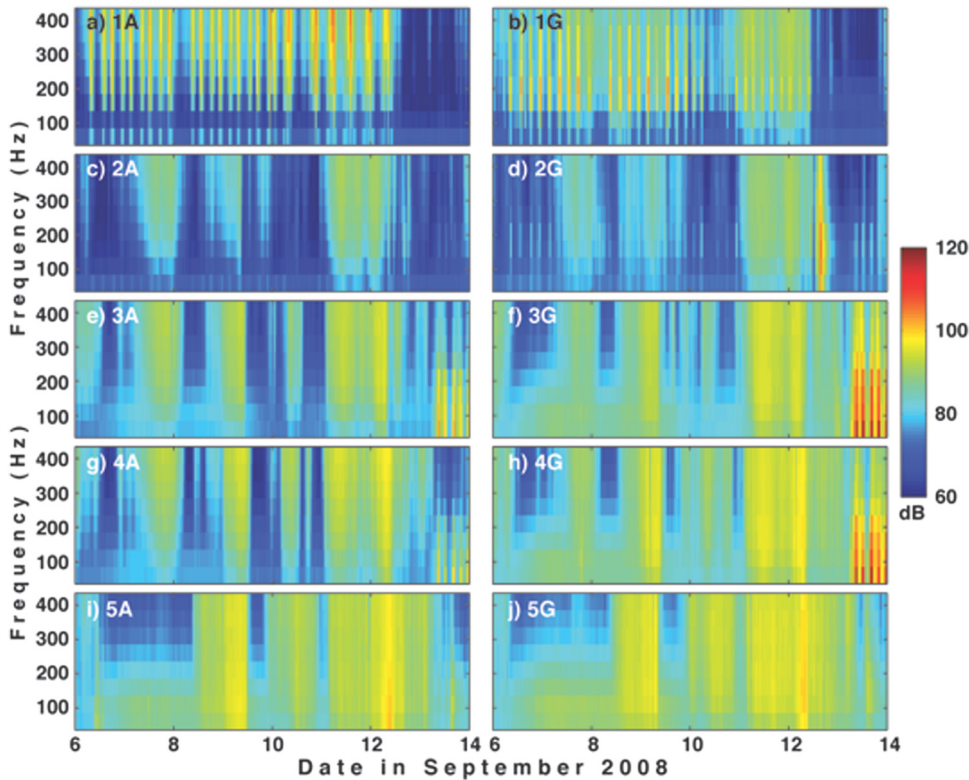


FIG. 7. (Color online) Expanded views of Figs. 5 and 6, covering seismic airgun activities between September 6th–14th. The left column plots the MLM (SPL units) of the shallowest DASAR at each site (A); the right column plots the metric for the deepest DASAR at each site (G). The rows correspond to the different sites and follow the format of Fig. 5.

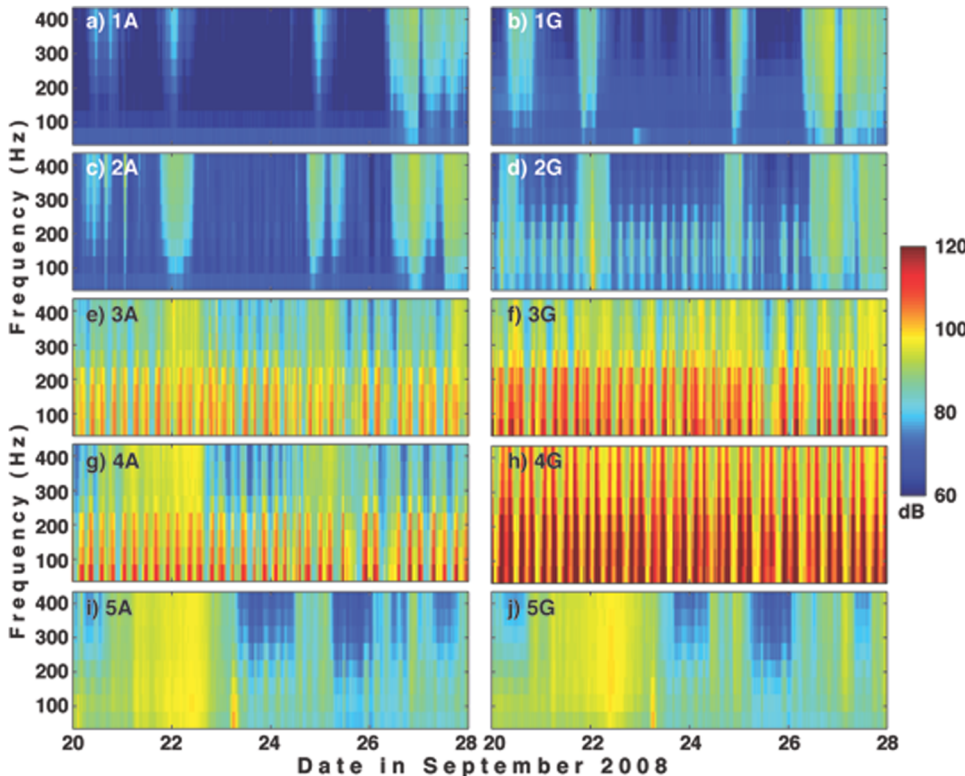


FIG. 8. (Color online) Expanded views of Figs. 5 and 6, covering seismic airgun activities between September 20th–28th during peak seismic airgun activity in close proximity to sites 3 and 4. The left column plots the MLM (SPL units) of the shallowest DASAR at each site (A); the right column plots the metric for the deepest DASAR at each site (G). The rows correspond to the different sites and follow the same order as the rows of Fig. 5.

and time offset between the wind and noise data. This matrix was used to determine the optimal time offset to apply to the regression model, which was +6 h, since at that time delay, the correlation coefficient is greatest for all frequency bands. Between 60 and 160 Hz the wind speed and MLM are highly correlated ($R^2_{\text{correlation}} = 0.8621$) with a 6 h time lag. Figure 9(c) shows that this correlation diminishes slightly at higher frequency ranges (i.e., $R^2_{\text{correlation}} = 0.7880$ at 360–460 Hz). Figure 9(d) plots the MLM between 60 and 160 Hz vs wind speed at the best time offset of +6 h, or where the MLM is advanced 6 h with respect to the wind times. This regression is re-computed for a total of eight 100-Hz frequency bands between 10 and 460 Hz.

Visual inspections of all the correlation plots across the DASARs suggested natural break points for three separate linear regressions that could be applied over three distinct regimes of wind speed: winds under 5 m/s [B_1], winds between 5–10 m/s [B_2], and winds exceeding 10 m/s [B_3]. Figure 9(d) shows the optimal linear regressions, although the third regression may not be valid as the number of data points available is small. A standardized Student's T test (Zar, 1984) was performed to establish the probability that such a fit would occur from a cloud of uncorrelated points. The resulting P values obtained from Fig. 9(d) are on the order of 8.8e–05, reflecting the low likelihood that the two variables are uncorrelated.

Figure 10(a) plots the two-dimensional MLM at DASAR 2A [Fig. 5(b)]. Figure 10(b) presents the modeled noise levels derived from applying the regression equations performed at each one of the eight frequency bands, like the one illustrated in Fig. 9(d), to the wind record in Fig. 9(b). In effect, remotely-sensed satellite data have been used to predict the temporal and spectral levels of the MLM [Fig.

10(b)]. The results of subtracting in dB-space (effectively, dividing) these modeled ambient noise levels from the MLM [Fig. 10(a)] creates Fig. 10(c), the RM, with units of dB SNR. Over this time period there was no detectable seismic airgun activity, so ideally, if wind alone explained ambient noise levels, the value of the metric should be 0 dB across all times and frequency ranges. The scatter of the points around the linear fit in Fig. 9(d), however, ensures that the RM will be nonzero even at times of no activity. The distribution of these non-zero fluctuations does not display a regular temporal pattern.

Finally, Fig. 11 shows the RM estimates for the same locations and time intervals shown in Fig. 8, computed for the shallowest and deepest DASAR at each of the five sites. The time scale covers September 20th–28th, 2008, a time of heavy seismic airgun survey activity occurring close to sites 3 and 4. The seismic airgun survey leaves distinctive, temporally regular signatures at DASARs in close proximity to the seismic airgun activity [e.g., Fig. 11(f) and 11(h)]. Figure 11 demonstrates the efficacy of the RM in quantifying the effects of seismic airgun reverberation on background noise in a shallow-water environment.

V. DISCUSSION

A. Minimum level metric (MLM) observations

The broadband MLM values in Fig. 3 indicate that the seismic airgun surveys generated sustained broadband changes in background noise levels while the survey took place. Two periods of substantial seismic airgun activity can be identified at sites 1 and 4 from the temporal pattern alone. In general, for DASARs within 10 km of the seismic airgun activities, the highest MLM values generated by the

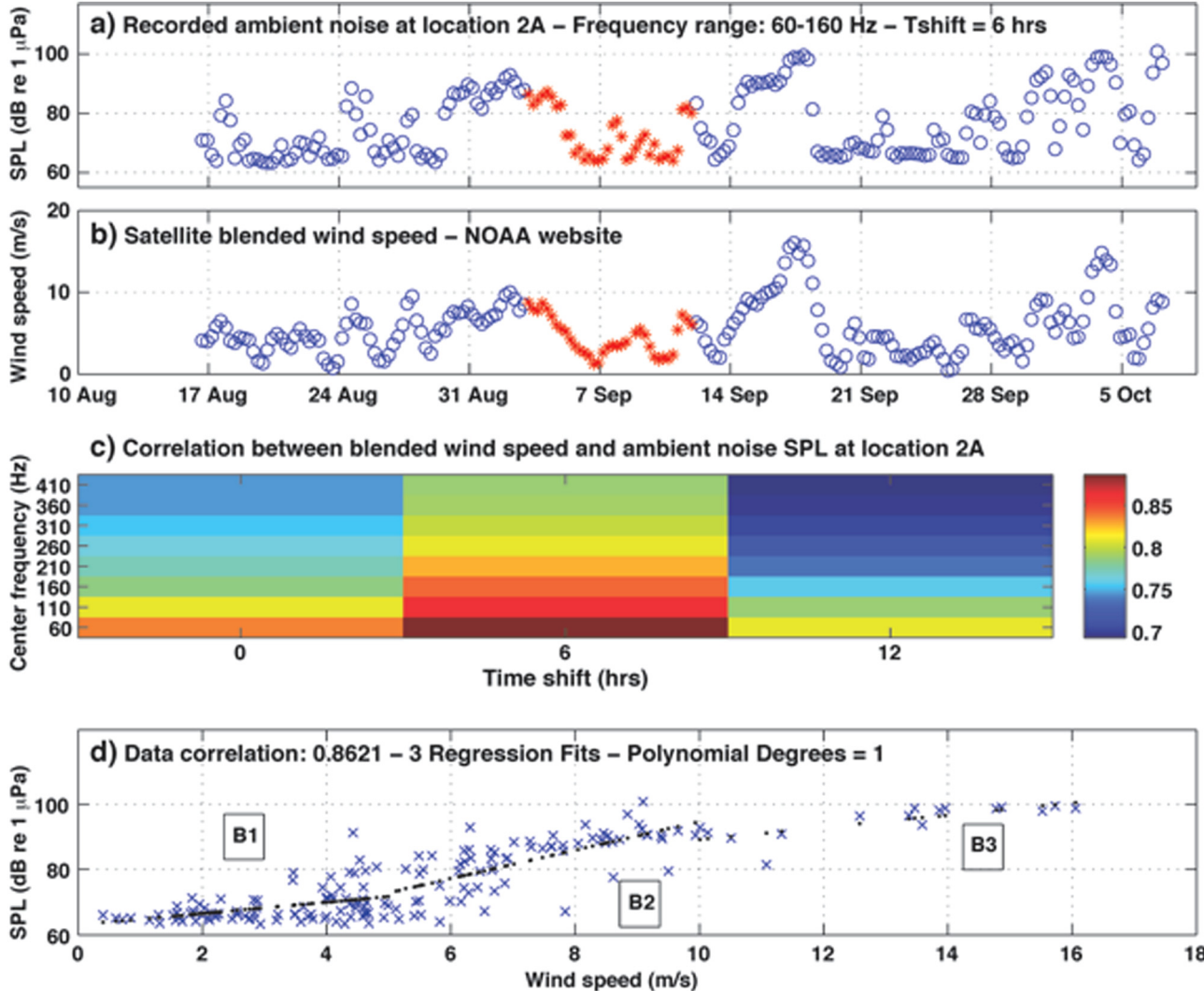


FIG. 9. (Color online) Relationship between MLM and wind speed databases: (a) MLM for DASAR 2A at 60–160 Hz, averaged over 6 h intervals; (b) blended wind speed time series in m/s, which consist of 6 h averages of wind speed around a $0.5^\circ \times 0.5^\circ$ grid surrounding the DASAR; (c) correlation coefficient between MLM (at DASAR 2A) and wind speed at different time delays and frequency ranges; (d) three linear regression fits between reverberation and wind. Corresponding slopes in dB/(m/s): $B_1 = 63.046 \pm 1.708$; $B_2 = 51.006 \pm 4.363$; $B_3 = 70.405 \pm 1.878$. Corresponding regression Student's test P -values: $P_1 = 1.9707e-05$; $P_2 = 1.2187e-10$; $P_3 = 2.4536e-04$.

reverberation matched or exceeded the MLM values attained during periods when seismic activity was absent. As expected, reverberation effects are greatest at DASARs closest to the activities; the shallowest DASAR at site 1 [Fig. 3(a)] and the deepest DASAR at site 4 [Fig. 3(d)].

Figures 5–8, which present the frequency and time dependence of the MLM at all five sites, reinforce these observations. Reverberation effects from airgun shots are again clearly recognizable, due to the “comb-like” pattern apparent in the MLM, which occurs because the seismic vessel rasters away and toward the recorder. For example, Figs. 8(f) and 8(h), centered on September 24th, demonstrate that MLM levels are high at site 4 when they are low at site 3, coinciding with the vessel traveling from site 3 toward site 4, and vice versa. Wind-driven changes in the MLM arising from changes in the ambient noise are seen to occur over longer time scales and over wider geographic areas, being recorded at multiple DASARs (e.g., the surge in ambient noise on September 9th in Fig. 7).

Airgun shots fired between sites 3 and 4, occurring between September 20th and 28th, produced the overall highest reverberation detected throughout the two-month period [Figs. 6(c), 6(d) and 8(f) and 8(h)]. Reverberation from this airgun activity can be observed on sites 4, 3 (up to 85 km away), and even at site 5 (93 km away) and site 2 (128 km away). The earlier seismic airgun survey between September 3rd and 12th had much weaker impacts on background noise levels beyond site 1, only influencing the deeper waters of site 2 (62 km away). Just as changes in water depth and/or bottom composition generate different reverberation effects (Fig. 2), these factors might also explain why reverberation decreases more rapidly with range at site 1, the shallowest of all the sites. As seen in Fig. 2(b), reverberation effects generated by the survey at site 1 had higher frequency content, relative to the later survey between sites 3 and 4 [Fig. 2(c)]. Since higher frequencies experience relatively greater propagation loss with range at shallow water depths between 25 and 50 m, it is not

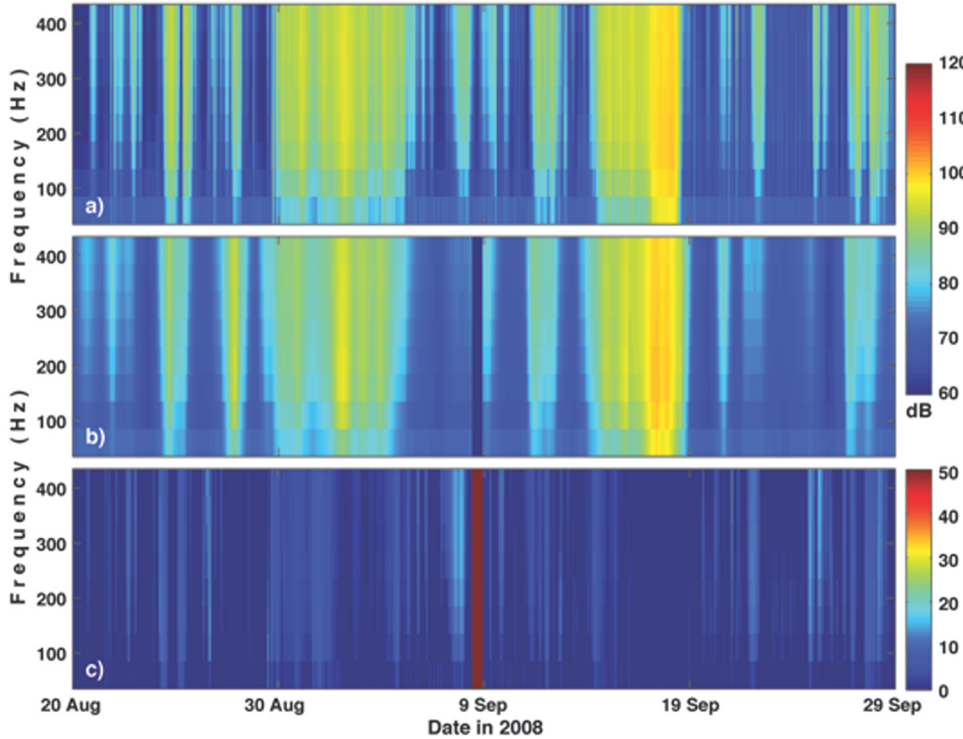


FIG. 10. (Color online) Example of reverberation metric (RM): (a) Time-frequency MLM for DASAR 2A; (b) time-frequency model of underwater wind noise from satellite observation data; (c) RM (ratio of measured to modeled MLM, or difference in dB). All units are shown in terms of dB intensity ratios. The red band represents times when satellite wind data are unavailable.

surprising that the reverberation effects from the site 1 survey decay much more quickly with range than the later surveys. It remains puzzling why site 5 is little affected by reverberation from the site 3/site 4 survey [Figs. 8(j) and 11(j)], compared with site 2 [Figs. 8(d) and 11(d)].

B. Wind driven ambient noise and the reverberation metric RM

Figure 9 illustrates the strong relationship between wind speed [Fig. 9(b)] and the MLM at DASAR 2A [Fig. 9(a)], which was distant to most seismic airgun activities. While Figs. 9(a) and 9(d) only show this relationship over a particular frequency band (60–160 Hz), Fig. 9(c) demonstrates that a correlation exists at all frequencies between 10 and 460

Hz, although the quality of the reverberation-wind correlation coefficient degrades with increasing frequency. The reverberation measurement times must be delayed 6 h with respect to the wind times to achieve the best correlation. These conclusions were verified by repeating the analysis using hourly wind data measurements from the Prudhoe Bay land-based weather station shown in Fig. 1. That analysis also found a high correlation between the MLM and wind speed and required a relative time delay of seven hours to maximize the correlation. The implication of these time shifts is that it takes ocean ambient noise levels about 6–7 h to respond to a change in wind speed.

A 6 h time shift was selected for regression analysis between the MLM and database wind speeds, and Fig. 9(d) shows an example of the set of linear regressions at one of

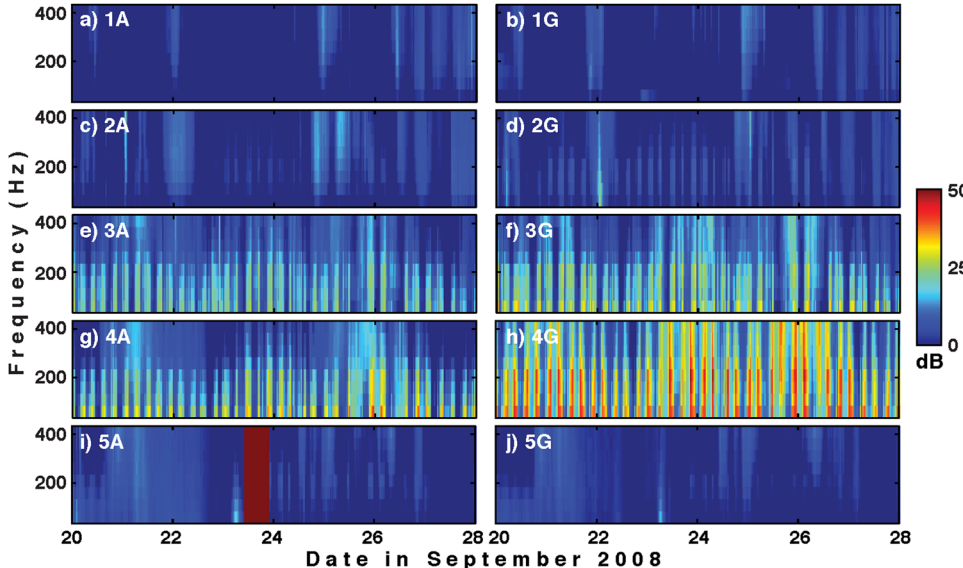


FIG. 11. (Color online) Expanded views of the RM covering seismic airgun activities between September 20th–28th. The left column plots the RM of the shallowest DASAR at each site and the right column plots the same metric for the deepest DASAR at each site. The rows correspond to different sites, and follow the same order as the rows of Figs. 7 and 8. Compare with Fig. 8, which shows the associated MLM.

the eight frequency ranges (60–160 Hz). Once all regression equations were computed for the corresponding eight frequency bands at every DASAR, all of them at a delay of 6 h, the MLM across all DASARs was modeled using the appropriate local wind time series. Figure 10(b) shows how the piecewise linear regressions capture much of the variability in the natural fluctuations of the MLM at site 2A [Fig. 10(a)], and thus the difference between the recorded and modeled MLM (i.e., the RM) suppresses large-scale natural ambient noise fluctuations [Fig. 10(c)]. Occasionally, short periods exist when local wind data were not available. These data “dropouts” result in blank regions, as occurs on September 9th in Figs. 10(b), 10(c). The fact that wind is the most significant contributor to ambient noise levels below 500 Hz is unusual; in most oceans, distant shipping noise dominates this band (Wenz, 1962). The absence of shipping noise in the low-frequency band of the Arctic acoustic environment may currently represent the closest oceanic scenario to pre-industrial ambient noise conditions.

When the RM is computed at all sites (Fig. 11), using specific regressions computed at each DASAR with satellite-derived wind speeds, the relative changes in the ambient noise levels due to patterns of airgun reverberation become clearly visible, e.g., at sites 2, 3, and 4, particularly in the deepest (northern) DASARs, at depths between 30 and 50 m [Figs. 11(d), 11(f), and 11(h)]. Thus, seismic airgun reverberation can produce measurable effects at distances of up to 128 km. Specifically, Fig. 11 indicates that at water depths of 50 m or less, seismic airgun activity within 1 km of a DASAR can increase noise levels by 30–45 dB over ambient levels (deep DASARs at sites 3 and 4), by 10–25 dB within 15 km range of the survey (shallow DASARs at sites 3 and 4), and by a few dB at ranges out to 128 km (site 2).

VI. CONCLUSION

Two metrics have been defined for characterizing reverberation from seismic airgun surveys in shallow water, which can complement standard metrics that focus on the coherent airgun pulse arrivals, such as the SPL and SEL. The minimum level metric (MLM) captures the minimum background sound level detected over a fixed time window, thus allowing it to capture long-term changes in background noise that arise *between* airgun pulses, while rejecting effects from dispersed modal and substrate transient arrivals. To compute the MLM three time-scale parameters were selected: a time over which to generate a single estimate of SE or SP, a time over which it is permissible to average sequential SE or SP estimates to reduce their variance, and a time over which the minimum value is selected. The MLM was applied to airgun signals recorded between 15 and 54 m depth in the Arctic Beaufort Sea in 2008. The resulting MLM shows that the spectral composition of reverberation is heavily dependent on receiving location, particularly water depth.

A second dimensionless metric, the reverberation metric (RM), can be derived from the MLM in various ways; in the results presented here, wind measurements were found to be highly correlated with the MLM over most frequency bands in the absence of seismic airgun activity. Thus the ambient

noise field was empirically modeled from satellite-derived wind speed estimates, and the dB levels of the models were subtracted from the MLM, yielding the RM. A RM of 0 dB would indicate that anthropogenic contributions to background levels are less than or equal to ambient contributions from other mechanisms. The RM indicates that the Gilavar shallow-water seismic airgun survey that took place between September 13th and 28th increased background noise levels by 30–45 dB over ambient levels within 1 km range of the survey, by 10–25 dB within 15 km range of the survey, and produced detectable modifications to background noise levels out to 128 km.

These results suggest that the range at which towed arrays or other PAM techniques would be effective for detecting the presence of marine mammal vocalizations within a few km of shallow-water seismic airgun surveys would be significantly reduced. This is because there is no time period between airgun shots when reverberation does not mask one’s ability to detect and recognize calls. The results here also suggest a potential for intraspecific communication masking, as defined in Clark *et al.* (2009), as a result of seismic airgun array activities.

These metrics provide a conservative, lower bound on reverberation levels, because reverberations that do not persist over the entire period between airgun shots are not included in the two metrics presented here. Equations (4) and (5) could be expanded to select not just minimum levels detected, but 25 and 50 percentile levels extracted from histograms of SEL and SPL derived from Eq. (3). This approach would permit detection and characterization of reverberation that exists for only a portion of time between impulses.

While percentile levels would add additional information about reverberation effects, the MLM defined here is convenient to compute, easy to understand and makes minimal biological assumptions about a particular species. Furthermore it could easily be incorporated into standard source level verification measurements of seismic airgun and other impulsive anthropogenic activities in shallow water. By these considerations, the potential communication masking effects of seismic airgun surveys on particular species of interest could be quantified. The inclusion of these metrics in monitoring and mitigation reports would also provide regulators with valuable insight into the expected efficacy of PAM and guide management strategies as relative to seismic surveys according to site-specific features of the environment.

ACKNOWLEDGMENTS

This work was supported by Shell Exploration and Production Company (SEPCO) and Greeneridge Sciences, Inc. (GSI). The second author received support from the North Pacific Research Board (NPRB). We are grateful to Charles R. Greene of GSI, for making this acoustic dataset available for analysis and for valuable suggestions on the manuscript. We thank Delphine Mathias and the entire crew of the R/V Norseman II for their help in the field collecting data. We also thank Chris Nations of WEST for informing us of the existence of the Blended Wind Data Set. We thank Bruce

Martin of JASCO and Ann E. Bowles of HSWRI for helpful and thoughtful comments on the manuscript.

- Barger, J. E., and Hamblen, W. R. (1980). "The air gun impulsive underwater transducer," *J. Acoust. Soc. Am.* **68**, 1038–1045.
- Blackwell, S. B., Norman, R. G., Greene, C. R., McLennan, M. W., and Richardson, W. J. (2006). "Acoustic monitoring of bowhead whale migration, autumn 2005," in *Monitoring of Industrial Sounds, Seals, and Bowhead Whales Near BP's Northstar Oil Development, Alaskan Beaufort Sea, 2005: Annual Summary Report*, edited by W. J. Richardson (LGL Ltd., King City, Ont.).
- Clark, C. W., Ellison, W. T., Southall, B. L., Hatch, L., Van Parijs, S. M., Frankel, A., and Ponirakis, D. (2009). "Acoustic masking in marine ecosystems: intuitions, analysis, and implication," *Mar. Ecol.: Prog. Ser.* **395**, 201–222.
- Clark, C. W., and Johnson, J. H. (1984). "The sounds of the bowhead whale, *Balaena mysticetus*, during the Spring migrations of 1979 and 1980," *Can. J. Zool.* **62**, 1436–1441.
- D'Spain, G. L., Hodgkiss, W. S., and Edmonds, G. L. (1991). "The simultaneous measurement of infrasonic acoustic particle-velocity and acoustic pressure in the ocean by freely drifting swallow floats," *IEEE J. Oceanic Eng.* **16**, 195–207.
- Di Iorio, L., and Clark, C. W. (2009). "Exposure to seismic survey alters blue whale acoustic communication," *Biol. Lett.* **6**, 51–54.
- Frisk, G. (1994). *Ocean and Seabed Acoustics: A Theory of Wave Propagation* (PTR Prentice Hall, Englewood Cliffs, NJ), pp. 89–172.
- Greene, C. R., McLennan, M. W., Norman, R. G., McDonald, T. L., Jakubczak, R. S., and Richardson, W. J. (2004). "Directional frequency and recording (DIFAR) sensors in seafloor recorders to locate calling bowhead whales during their fall migration," *J. Acoust. Soc. Am.* **116**, 799–813.
- Greene, C. R., and Richardson, W. J. (1988). "Characteristics of marine seismic survey sounds in the Beaufort sea," *J. Acoust. Soc. Am.* **83**, 2246–2254.
- Ireland, D. S., Funk, D. W., Rodrigues, R., and Koski, W. R. (2009). "Joint Monitoring Program in the Chukchi and Beaufort seas, open water season, 2006–2007," in *LGL Alaska Report P971-2* (LGL Ltd., Environmental Research Associates, King City, Ont., JASCO Research Ltd., Victoria, BC, and Greeneridge Sciences, Inc., Santa Barbara, CA, for Shell Offshore, Inc. Anchorage, AK, ConocoPhillips Alaska, Inc., Anchorage, AK, and the National Marine Fisheries Service, Silver Springs, MD, and the U.S. Fish and Wildlife Service, Anchorage, AK., Anchorage, AK).
- Kastak, D., Southall, B. L., Schusterman, R. J., and Kastak, C. R. (2005). "Underwater temporary threshold shift in pinnipeds: Effects of noise level and duration," *J. Acoust. Soc. Am.* **118**, 3154–3163.
- Ljungblad, D. K., Leatherwood, S., and Dahlheim, M. E. (1980). "Sounds recorded in the presence of an adult and calf bowhead whale," *Mar. Fisheries Rev.* **42**, 86–87.
- Madsen, P. T. (2005). "Marine mammals and noise: Problems with root mean square sound pressure levels for transients," *J. Acoust. Soc. Am.* **117**, 3952–3957.
- Oppenheim, A. V., Schafer K., Ronald W., Buck, John R. (1975). *Digital Signal Processing* (Prentice Hall, Englewood Cliffs, NJ), pp. 548–554.
- Richardson, W. J., Würsig, B., and Greene, C. R. (1986). "Reactions of bowhead whales, *Balaena mysticetus*, to seismic exploration in the Canadian Beaufort sea," *J. Acoust. Soc. Am.* **79**, 1117–1128.
- Southall, B. L., Bowles, A. E., Ellison, W. T., Finneran, J. J., Gentry, R. L., Greene, C. R., Jr., Kastak, D., Ketten, D. R., Miller, J. H., Nachtigall, P. E., Richardson, W. J., Thomas, J. A., and Tyack, P. L. (2007). "Marine mammal noise exposure criteria: Initial scientific recommendations," *Aquat. Mamm.* **33**, 1–521.
- Urick, R. J. (1983). *Principles of Underwater Sound* (McGraw-Hill, New York), pp. 1–423.
- Wenz, G. M. (1962). "Acoustic ambient noise in the ocean: spectra and sources," *J. Acoust. Soc. Am.* **334**, 1936–1956.
- Yost, W.A. (1994). *Fundamentals of Hearing: An Introduction* (Academic Press, San Diego), pp. 1–326.
- Young, I. M., and Wenner, C. (1970). "Two distinct loudness functions of the ear," in *79th Meeting of the Acoustical Society of America* (Acoustical Society of America, Atlantic City, NJ), pp. 7.
- Zar, J. H. (1984). *Biostatistical Analysis*, 2nd ed. (Prentice-Hall, Engelwood Cliffs, NJ), pp. 97–121.
- Zhang, H. M., Bates, J. J., and Reynolds, R. W. (2006). "Assessment of composite global sampling: Sea surface wind speed," *Geophys. Res. Lett.* **33**, L17714.